

Deep Learning Based Signal Enhancement of Low-Resolution Accelerometer for Fall Detection Systems

Kai-Chun Liu, Kuo-Hsuan Hung, Chia-Yeh Hsieh, Hsiang-Yun Huang, Chia-Tai Chan, and Yu Tsao

Abstract— In the last two decades, fall detection (FD) systems have been developed as a popular assistive technology. Such systems automatically detect critical fall events and immediately alert medical professionals or caregivers. To support long-term FD services, various power-saving strategies have been implemented. Among them, a reduced sampling rate is a common approach for an energy-efficient system in the real-world. However, the performance of FD systems is diminished owing to low-resolution (LR) accelerometer signals. To improve the detection accuracy with LR accelerometer signals, several technical challenges must be considered, including misalignment, mismatch of effective features, and the degradation effects. In this work, a deep-learning-based accelerometer signal enhancement (ASE) model is proposed to improve the detection performance of LR-FD systems. This proposed model reconstructs a high-resolution (HR) signal from the LR signal by learning the relationship between the LR and HR signals. The results show that the FD system using support vector machine and the proposed ASE model at an extremely low sampling rate (sampling rate < 2 Hz) achieved 97.34% and 90.52% accuracies in the SisFall and FallAID datasets, respectively, while those without ASE models only achieved 95.92% and 87.47% accuracies in the SisFall and FallAID datasets, respectively. This study demonstrates that the ASE model helps the FD systems tackle the technical challenges of LR signals and achieve better detection performance.

Index Terms— Low-resolution fall detection, accelerometer signal enhancement, deep learning approach, wearable sensors

I. INTRODUCTION

Falls are a leading cause of major injuries and deaths among the aging population. The world health organization [1] reported that more than 30% of the elderly, aged over 64 years, fall at least once a year. Approximately half of them were unable to get back up without assistance due to fall-related injuries or a lack of physical fitness and strength [2]. A previous study has shown that 50% of the elderly population died within 6 months of the fall event because they were lying on the floor for more than an hour [3].

In the past two decades, automatic fall detection (FD) systems have been developed as an assistive technology [4]. The main goal of FD systems is to automatically detect critical

fall events and immediately alert medical professionals or caregivers [4-6]. Moreover, this systems can relieve the psychological stress affecting elders and caregivers [7].

Owing to advancements in information communication technologies and body sensor networks, various sensor technologies have been used in FD systems including inertial sensors [6], depth-cameras [8], microphones [9], pressure sensors [10], and thermal sensors [11]. In particular, accelerometers are the most common sensors for FD, which capture body movements and are sensitive to posture changes. FD systems using accelerometers have advantages such as compactness, low cost, effectiveness, unobtrusiveness, and high mobility [12].

Wearable sensors must be placed on the body and function as long as possible to enable long-term FD services. This demand leads to challenges in design and development of systems, including reliability, security, usability, and sustainability [13]. For instance, the number of batteries would impact the size and comfortability of sensors [14]. Furthermore, recharging or replacing batteries frequently may decrease its usability [15] and the user's acceptance of the FD system [16]. Therefore, several energy-efficient FD systems that focus on reducing power consumption and extending battery life have been developed for long-term FD services.

In a typical FD system, measurement devices (e.g., wrist-band and smartwatches) send the collected data wirelessly to a processing unit (e.g., smartphones, laptops, and work stations) for identifying a fall event. Factors such as sampling rate, feature extraction and selection, communication protocol, detector design, and utilization of low-power electronic components [17-22] influence the power consumption in FD systems. Most studies adjust or optimize the sampling rates for power-efficient FD systems. This is because at high sampling rates, up to 90% of the power consumption of wearable health monitoring systems is owing to data sampling [23, 24]. Moreover, lesser the data collected, the lesser the data transfer volume. This could reduce the power consumption in FD systems.

Wang *et al.* [17] proposed a power-saving framework that switch from a low-power mode with the sampling rate of 6 Hz to the measurement mode at 50 Hz when the possible fall event is triggered. In addition, previous studies [19, 20] explored the effects of the sampling rate on the detection performance of low-power FD systems. These studies reported that the detection accuracy of FD systems is sensitive to sampling rates [19, 20]. In particular, the accuracy decreases significantly when the sampling rate is less than 10 Hz [20]. This is because low sampling leads to low-resolution (LR) accelerometer

Manuscript received October xx; revised xx; accepted xx. Date of publication xx; date of current version xx. This work was supported in part by grants from the Ministry of Science and Technology MOST

K.-C. Liu, K.-H. Hung, and Y. Tsao are with the Research Center for Information Technology Innovation, Academia Sinica, Taipei 11529, Taiwan

C.-Y. Hsieh, H.-Y. Huang and C.-T. Chan are with the Department of Biomedical Engineering, National Yang-Ming University, Taipei 11221, Taiwan.

(Corresponding author: Yu Tsao, e-mail: yu.tsao@citi.sinica.edu.tw).

signals for FD systems.

Improving the detection accuracy of FD systems using LR accelerometer signals requires the consideration of technical challenges. The first challenge is the *misalignment*. The event-defined window is a popular approach for FD systems that use high-resolution (HR) accelerometer signals [6, 25, 26]. This approach detects the impact point to determine the entire fall event. However, inaccurate alignment of the impact point might occur when using LR accelerometer signals and negatively affect the FD performance. The second challenge is the *mismatch of effective features*. LR accelerometer signals lead to a loss in fine-grained movement information. The feasible features used in FD systems that are trained using HR signals cannot perform well when LR signals are processed. In other words, additional efforts are required to explore the *efficient features* of LR-FD models. The last one is the *degradation effects*. The critical fall characteristics including free-fall, impact, vibration, and recovery are degraded in low-quality signals. Such degradation makes it difficult to tackle classification problems (e.g., inter-class ambiguity and intra-class variability).

In this study, we propose a deep learning (DL)-based accelerometer signal enhancement (ASE) approach to tackle the aforementioned challenges in LR-FD systems. We use the DL-based ASE model to reconstruct HR signals from LR signals. The reconstructed HR signals are then fed to the FD system. FD systems can yield higher detection accuracy with reconstructed HR signals.

The main contributions of this work are as follows:

- A DL-based ASE model, based on a deep denoising autoencoder architecture, is proposed to reconstruct HR accelerometer signals from LR ones.
- We comprehensively analyze the DL-based ASE model on a wearable FD system and a typical FD model to measure the detection performance, which varies with different sampling rates.
- Two emulated public fall detection datasets were employed to validate the effectiveness of the proposed ASE model for achieving a higher detection accuracy.

The remainder of this paper is organized as follows. Section II introduces the selected open datasets and their experimental protocols. In Section III, we describe the design principles and mechanisms of the proposed ASE model for FD systems. The results of the experiment with the proposed FD system are presented in Section IV. The comprehensive performance analysis of the ASE model for FD systems, its limitations, and future works are discussed in Section V. Finally, we conclude this study in Section VI.

II. OPEN DATASETS

Currently, open datasets for wearable FD including SisFall [27], FallAIID [28], UMAFall [29], and UPFall [30] are available. In this study, SisFall and FallAIID datasets are used to validate the effectiveness of the proposed DL-based ASE

model on the LR-FD. Compared to other datasets, these two datasets with diverse fall types and activities of daily living (ADL) are more challenging and closer to the real-world situation. In addition, these datasets use accelerometers with a sampling rate of at least 200 Hz. This may contrast the effects of the proposed model with different resolution accelerometer signals from HR signals to LR signals.

A. FallAIID dataset

The FallAIID dataset proposed by Saleh and Jeannes [28] was used in this study. An inertial measurement unit (IMU) was placed on the neck, chest, and waist, respectively, to measure the movement during the experiment. Each inertial sensor unit includes a tri-axial accelerometer (sampling rate: 238 Hz, range: ± 8 g), tri-axial gyroscope (sampling rate: 238 Hz, angular rate: ± 2000 dps), tri-axial magnetometer (sampling rate: 80 Hz, range: ± 4 G), and a barometer (sampling rate: 10 Hz). A previous study [26] showed that the FD system using a waist-worn accelerometer is better than those in other positions. Therefore, we focus on the collected accelerometer data from the waist.

The experimental data were collected from 15 healthy young subjects (8 males and 7 females). Their average age, height, and weight were 32 years, 171 cm, and 67 kg, respectively. We only used the data from 10 subjects that performed falls and ADL. In total, there were 1053 ADL and 423 fall instances. TABLE I and TABLE II lists the detailed ADL and fall types, respectively.

B. SisFall dataset

The SisFall dataset [27] involves two age groups: 15 elder healthy subjects and 23 young healthy subjects. This study employs the raw data collected from 21 young subjects (10 males, 11 females, age 25.0 ± 8.6 years, height 165.7 ± 9.3 cm, weight 57.7 ± 15.5 kg) for the experiment. A group of elder people were not considered in this study because they were not made to fall in these experiments. In addition, two young adults were excluded owing to their incomplete ADL trials. There were 1575 fall and 1659 ADL instances. The details of the involved falls and ADLs are listed in TABLE III. An IMU (Shimmer, Ireland) placed on the waist captured the motion data at a sampling rate of 200 Hz. The proposed model only explores the data collected from accelerometers, while the sensor consists of accelerometers and gyroscopes.

C. Downsampling

The downsampling approach is employed to obtain LR signals from HR signals for exploring the effects of different resolutions on the FD performance. The LR signal S^{LR} is gathered by applying downsampling approaches to the HR signal $S^{HR} = \{s_j | j = 1, 2, \dots, n_{HR}\}$ by an integr factor n , which is defined as follows:

$$S^{LR} = \{s_k | k = 1 + 2^\alpha \times n\}, \quad (1)$$

where it keeps the first sample from every 2^α sample, $0 \leq n \leq$

TABLE I
THE TYPES OF ADLS IN FALLALLD DATASET.

Type of ADLs	Trials	Type of ADLs	Trials
A13 sitting down	110	A29 start going upstairs	20
A14 standing up	113	A30 going upstairs	20
A15 fail to stand up from a sofa/chair	31	A31 stop going upstairs	20
A16 lying down on a bed	57	A32 start going downstairs	20
A17 changing position (turning) in the bed	51	A33 going downstairs	20
A18 rising up from a bed	55	A34 stop going downstairs	20
A19 start walking	43	A35 going upstairs quickly	20
A20 walking slowly or in moderate speed	43	A36 going downstairs quickly	20
A21 stop walking	42	A37 start ascending using a lift	20
A22 walking quickly	27	A38 stop ascending using a lift	20
A23 stumbling while walking without falling	21	A39 start descending using a lift	20
A24 jogging slowly	17	A40 stop descending using a lift	20
A25 jogging quickly	18	A41 standing in a moving bus/metro	21
A26 jumping slightly	34	A42 sitting in a moving bus/metro	15
A27 jumping strongly	36	A43 start jogging	21
A28 bending down	36	A44 stop jogging	22

TABLE II
THE TYPES OF FALLS IN FALLALLD DATASET.

Pre-fall Activity	Reasons of fall	Fall direction	Rotation ?	Recovery ?	Trials
F01 walking	stumbling/tripping	forward	no	no	13
F02 walking	stumbling/tripping	forward	no	yes	12
F03 walking	slipping	forward	no	no	12
F04 walking	slipping	forward	no	yes	11
F05 walking	slipping	forward	yes	no	18
F06 walking	slipping	forward	yes	yes	15
F07 walking	slipping	backward	no	no	23
F08 walking	slipping	backward	no	yes	22
F09 walking	slipping	backward	yes	no	17
F10 walking	slipping	backward	yes	yes	15
F11 walking	fainting/syncope	backward	no	no	7
F12 walking	fainting/syncope	backward	no	no	6
F13 walking	fainting/syncope	lateral	no	no	15
F14 walking	fainting/syncope	forward	no	no	14
F15 attempting to sit/lie down	losing balance	forward	no	no	5
F16 attempting to sit/lie down	losing balance	forward	no	yes	6
F17 attempting to sit/lie down	losing balance	backward	no	no	4
F18 attempting to sit/lie down	losing balance	backward	no	yes	6
F19 attempting to sit/lie down	losing balance	lateral	no	no	12
F20 attempting to sit/lie down	losing balance	lateral	no	yes	14
F21 jogging	stumbling/tripping	forward	no	no	15
F22 jogging	stumbling/tripping	forward	no	yes	11
F23 jogging	slipping	forward	no	no	15
F24 jogging	slipping	forward	no	yes	13
F25 jogging	slipping	forward	yes	no	17
F26 jogging	slipping	forward	yes	yes	13
F27 lying in bed	changing position/rotating	lateral	no	no	20
F28 lying in bed	changing position/rotating	lateral	no	no	15
F29 sitting on a chair	fainting/syncope	forward	no	no	7
F30 sitting on a chair	fainting/syncope	backward	no	no	4
F31 sitting on a chair	fainting/syncope	lateral	no	no	12
F32 standing for a while	fainting/syncope	forward	no	no	7
F33 standing for a while	fainting/syncope	backward	no	no	4
F34 standing for a while	fainting/syncope	lateral	no	no	12

TABLE III
THE TYPES OF FALLS AND ADLS IN SISFALL DATASET.

Type of Falls	Trials
F01 Fall forward while walking, caused by a slip	105
F02 Fall backward while walking, caused by a slip	105
F03 Lateral fall while walking, caused by a slip	105
F04 Fall forward while walking, caused by a trip	105
F05 Fall forward while jogging, caused by a trip	105
F06 Vertical fall while walking, caused by fainting	105
F07 Fall while walking, with use of hands on a table to dampen fall, caused by fainting	105
F08 Fall forward when trying to get up	105
F09 Lateral fall when trying to get up	105
F10 Fall forward when trying to sit down	105
F11 Fall backward when trying to sit down	105
F12 Lateral fall when trying to sit down	105
F13 Fall forward while sitting, caused by fainting or falling asleep	105
F14 Fall backward while sitting, caused by fainting or falling asleep	105
F15 Lateral fall while sitting, caused by fainting or falling asleep	105
Activities of Daily Living (ADLs)	
A01 Walking slowly	21
A02 Walking quickly	21
A03 Jogging slowly	21
A04 Jogging quickly	21
A05 Walking upstairs and downstairs slowly	105
A06 Walking upstairs and downstairs quickly	105
A07 Slowly sitting in a half-height chair, waiting a moment, and standing up slowly	105
A08 Quickly sitting in a half-height chair, waiting a moment, and standing up quickly	105
A09 Slowly sitting in a low-height chair, waiting a moment, and standing up slowly	105
A10 Quickly sitting in a low-height chair, waiting a moment, and standing up quickly	105
A11 Sitting a moment, trying to get up, and collapsing into a chair	105
A12 Sitting a moment, lying slowly, waiting a moment, and sitting again	105
A13 Sitting a moment, lying quickly, waiting a moment, and sitting again	105
A14 Being on one's back, changing to lateral position, waiting a moment, and changing to one's back	105
A15 Standing, slowly bending at the knees, and getting up	105
A16 Standing, slowly bending without bending knees, and getting up	105
A17 Standing, getting into a car, remaining seated, and getting out of the car	105
A18 Stumbling while walking	105
A19 Gently jumping without falling, while trying to reach a high object	105

$\frac{L-1}{2^\alpha}$, and n_{HR} is the total number of samples in S^{HR} . The corresponding downsampling rate of the LR signal is $R/2^\alpha$ Hz, where the original sampling rate of the HR accelerometer signal is R Hz. In this study, an integer factor ranging from $\alpha = 1, 2, \dots, 7$ is applied to the SisFall and FallAllD datasets.

III. METHODOLOGY

This study develops an FD system with a DL-based ASE model as a front-end processor for FD using LR accelerometer signals. The overall system consists of the pre-processing unit, the ASE unit, and the FD unit. Initially, a series of signal processing processes are applied to the raw LR accelerometer signal S^{LR} , involving impact-defined window and min-max normalization. Then, the network architecture of the proposed deep ASE model is introduced, which involves feed-forward convolutional neural networks and deep neural networks. The main goal of ASE model is to enhance the LR accelerometer signals and generate HR signals. Finally, the classical FD model is applied to the enhanced signal to classify the fall and ADL.

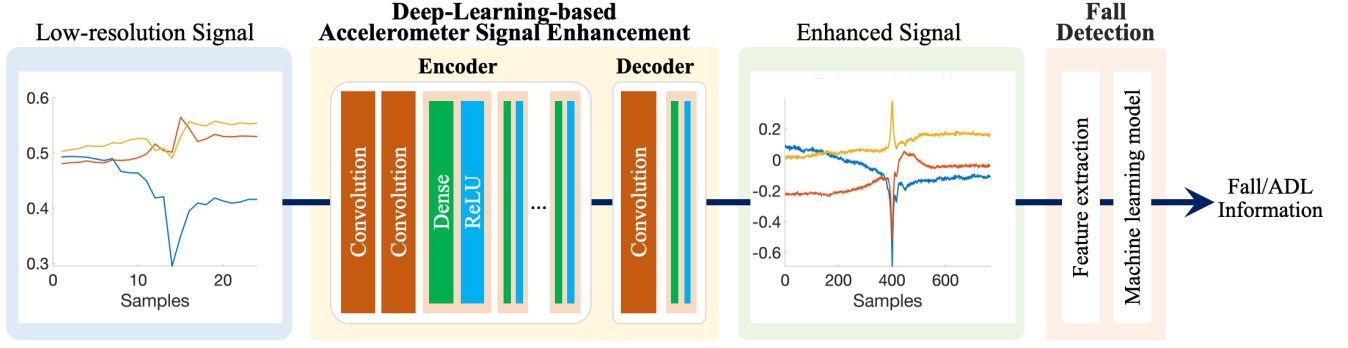


Fig. 1 The framework of the proposed DL-based ASE for FD systems

A. Pre-processing

1) Impact-defined window

The impact-defined windowing approach processes the LR accelerometer signal. This ensures that the entire critical fall event is fully covered in a window. Given that an input accelerometer signal is defined as $S = \{s_j | j = 1, 2, \dots, n_s\}$, where n_s is the total number of samples in the trial. The sample point involves the three-dimensional acceleration $s_j = \{a_{x_j}, a_{y_j}, a_{z_j}\}$. First, the data sample with the maximum $Norm_{xyz}$ is considered as the impact sample point s_l of the instance, where $Norm_{xyz}$ of s_j is calculated by Equation (2). Next, based on the s_l , forward and backward sub-windows are determined as $W_f = \{s_{l+1}, \dots, s_{l+WS_f-1}, s_{l+WS_f}\}$ and $W_b = \{s_{l-WS_b}, s_{l-WS_b+1}, \dots, s_{l-1}\}$, respectively. Here, WS_f and WS_b are the window sizes of W_f and W_b , respectively. Details of the impact-defined window approach are introduced in [6, 25, 26].

$$Norm_{xyz}(s_j) = \sqrt{a_{x_j}^2 + a_{y_j}^2 + a_{z_j}^2} \quad (2)$$

WS_f and WS_b are determined as 2s and 1.44s, respectively for the SisFall dataset, and 2s and 1.23s, respectively for the FallAID dataset. A previous study has shown that FD systems with window sizes can achieve the best system performance [25].

2) Min-max normalization

After the impact-defined window, a min-max normalization is utilized to process the data. This approach can reduce scaling effects on the deep ASE model during the training phase. Given a data sequence $S = \{s_j | i = 1, 2, \dots, n_s\}$, s_i can be normalized to the range [0,1] using min-max normalization, as shown in Equation (3):

$$s_j^{nom} = \frac{s_j - s_{min}}{s_{max} - s_{min}}, \quad (3)$$

where s_{max} and s_{min} are the maximum and minimum values of S , respectively.

B. DL-based accelerometer signal enhancement.

1) Network Architecture of ASE

The framework of the proposed ASE model for FD systems

is shown in Fig. 1. The over-model is a deep denoising autoencoder architecture, which consists of an encoder and decoder that contain convolution layers and dense layers.

First, the encoder convolution layer (ECL) captures movement features from a tri-axial accelerometer signal. Each ECL includes two convolution layers, consisting of $5 * (8 - \log_2(\frac{O}{D}))$ filters with a filter size of 3, where O and D are the sampling rates of the HR and LR signals, respectively. Then, the encoder dense layer reconstructs the HR signal from the LR signal. The encoder dense layer consists of 5 to 8 layers. Finally, the decoder adjusts the encoder output to be similar to the original data. All decoder convolution layers in the ASE model have a filter of size 3. All dense layers employ rectified linear units (ReLU) as the activation function for the hidden layers. There are no activation functions in the convolution layers. The details of the ASE models at different sampling rates are shown in Table IV.

2) Training strategy

Given that the preprocessed HR and LR accelerometer signals are defined as $S^{HR} = \{s_1^{HR}, s_2^{HR}, \dots, s_N^{HR}\}$ and $S^{LR} = \{s_1^{LR}, s_2^{LR}, \dots, s_M^{LR}\}$, respectively, where $N \geq 2^a \times M$, we use LR-HR signal pairs to train the ASE model. The enhanced accelerometer signals $S^E = \{s_1^E, s_2^E, \dots, s_N^E\}$ are represented as:

$$S^E = f_{decoder}(f_{encoder}(S^{LR})), \quad (4)$$

where $f_{encoder}$ and $f_{decoder}$ denote the encoder and decoder functions, respectively. The mean absolute error (MAE) is used as the objective function, and the loss function is formulated as:

$$loss = \frac{1}{N} \sum_{j=1}^N |s_j^{HR} - s_j^E|, \quad (5)$$

where s_j^{HR} , s_j^E denotes the HR signal and the enhanced signal, respectively, and N denotes the number of training sets. The ASE model is trained by K-fold cross-validation with the same data in the FD. The training data is divided into a training set and a validation set at a ratio 9:1. In the encoder, the layer numbers are set according to the sampling rate. This is because the lower sampling rate offers less information than higher sampling rate. Therefore, fewer filter numbers are sufficient for feature extraction through the ASE model. Note that the pooling layer and dropout are not used in the model.

TABLE IV
THE IMPLEMENTATION DETAIL OF THE PROPOSED ASE MODEL FOR DIFFERENT SAMPLING RATES.

Sampling Rates (Hz)		Encoder Convolution layer				Encoder Dense layer		Decoder Convolution layer			Decoder Dense layer	
SisFall	FallAIIID	Input size	Layers	Filter size	Output channel	Layers	Hidden units	Layers	Filter size	Output channel	Layers	Hidden units
200	238.00	768	2	3x3	40	5	[768,768,768,768,768]	1	3x3	1	1	768
100	119.00	384	2	3x3	35	6	[384,384,384,384,768,768]	1	3x3	1	1	768
50	59.50	192	2	3x3	30	6	[192,192,192,384,768,768]	1	3x3	1	1	768
25	29.75	96	2	3x3	25	8	[96,96,96,96,192,384,768,768]	1	3x3	1	1	768
12.5	14.88	48	2	3x3	20	8	[48,48,48,96,192,384,768,768]	1	3x3	1	1	768
6.25	7.44	24	2	3x3	15	8	[24,24,48,96,192,384,768,768]	1	3x3	1	1	768
3.13	3.72	12	2	3x3	10	8	[12,24,48,96,192,384,768,768]	1	3x3	1	1	768
1.56	1.86	6	2	3x3	5	8	[12,24,48,96,192,384,768,768]	1	3x3	1	1	768

C. FD model

1) Feature extraction

Feature extraction aims to obtain effective parameters that can classify ADL and fall events. The FD model utilizes eight one-dimensional and one three-dimensional statistical features to enhance the accelerometer signal including mean, standard deviation (STD), variance, maximum, minimum, range, kurtosis, skewness, and correlation coefficient. These features are calculated through Equations (6) – (14):

$$\text{mean}(S^E): \mu = \frac{1}{N} \sum_{i=1}^N s_i^E, \quad (6)$$

$$\text{STD}(S^E): \sigma = \sqrt{\frac{1}{N} \sum_{i=1}^N (s_i^E - \mu)^2}, \quad (7)$$

$$\text{Variance}(S^E): \frac{1}{N} \sum_{i=1}^N (s_i^E - \mu)^2, \quad (8)$$

$$\text{Maximum}(S^E): x_{MAX} = \max_{i=1,2,\dots,N} s_i^E, \quad (9)$$

$$\text{Minimum}(S^E): x_{MIN} = \min_{i=1,2,\dots,N} s_i^E, \quad (10)$$

$$\text{Range}(S^E): x_{MAX} - x_{MIN}, \quad (11)$$

$$\text{Kurtosis}(S^E): \frac{1}{N\sigma^4} \sum_{i=1}^N (s_i^E - \mu)^4, \quad (12)$$

$$\text{Skewness}(S^E): \frac{1}{N\sigma^3} \sum_{i=1}^N (s_i^E - \mu)^3, \quad (13)$$

$$\text{Corr}(Y, Z): \frac{1}{N-1} \sum_{i=1}^N \left(\frac{Y_i - \mu_Y}{\sigma_Y} \right) \left(\frac{Z_i - \mu_Z}{\sigma_Z} \right), \quad (14)$$

where μ , σ , x_{MAX} and x_{MIN} are the mean, standard deviation, maximum and minimum of the sequence, respectively. The Y and Z are any two sequences, μ_Y and σ_Y are the mean and standard deviation of Y , respectively, and μ_Z and σ_Z are the mean and standard deviation of Z , respectively. These features have been used in various accelerometer-based health applications such as fall detection [6], drinking event identification [31], and housekeeping task recognition [32]. There are 54 features gathered from S^E and applied to machine learning models.

2) Machine learning model

Two machine learning classification algorithms were utilized to analyze the effects of the DL-based ASE model on the LR-FD systems: support vector machine (SVM) and k-nearest neighbor (k -NN). These classification algorithms are classical models in the field of wearable FD systems. Previous studies have shown that the selected algorithms are the most reliable, compared to other common machine learning models (e.g., naïve Bayes and decision tree), for FD systems [6, 25, 26, 33]. Brief introductions of these classification algorithms are as follows:

- **SVM**: Generally, the SVM model distinguishes target classes with maximum margins based on the hyperplane optimization. The input data are mapped onto a new dimensional space. Then, the decision boundary is determined by finding the largest possible margin between the points of the different classes. Finally, the SVM model classifies the testing data according to the decision boundary. In this study, a radial basis function (RBF) kernel is employed for the SVM.

- **k -NN classifier**: Known also as the lazy classifier, is a typical instance-based classification model. This classification mainly relies on majority voting among the k -nearest training samples to the testing sample. The Euclidean distance is also taken into account for the weight of the neighbors. Previous studies [21, 27] have shown that the classical FD system has the best detection accuracy with $k = 3$. Therefore, 3-NN is employed to classify fall/ADL in this study.

D. Performance Evaluation

The leave-one-subject-out (LOSO) cross-validation approach is introduced to validate the FD systems. Four evaluation metrics, namely accuracy (ACC), sensitivity (SEN), specificity (SPE), and precision (PRE), were introduced to measure the detection performance. These metrics are defined in Equations (15)–(18):

$$\text{ACC} = \frac{TP+TN}{TP+FP+TN+FN}, \quad (15)$$

TABLE V

THE BEST PERFORMANCE USING TYPICAL WEARABLE FD SYSTEMS WITH AND WITHOUT THE ASE MODEL IN SISFALL DATASET (%).

	kNN	original kNN	enhanced SVM	original SVM	enhanced
Accuracy	98.70	99.07	98.95	99.41	
Sensitivity	98.22	99.11	99.24	99.56	
Specificity	99.22	99.04	98.79	99.34	
Precision	99.17	98.99	98.73	99.30	

$$SEN = \frac{TP}{TP+FN}, \quad (16)$$

$$SPE = \frac{TN}{TN+FP}, \quad (17)$$

$$PRE = \frac{TP}{TP+FP}, \quad (18)$$

where true positive (TP), true negative (TN), false positive (FP), and false negative (FN) are cases where the labeled fall signal is recognized as a fall, the labeled ADL signal is recognized as an ADL, the labeled ADL signal is recognized as a fall, and the labeled fall signal is recognized as an ADL, respectively.

The accelerometer signal enhancement model was implemented through PyTorch 1.3.1, running on a workstation with 64 bit Ubuntu 18.04.4, Intel(R) Xeon(R) Gold 6152 CPU @ 2.10GHz, and trained and tested using the Nvidia GTX 2080Ti with 11 GB dedicated memory. The pre-processing and fall detection processes are realized using the Statistics and Machine Learning Toolbox in the MATLAB 2016 environment.

IV. EXPERIMENTAL RESULTS

In this study, typical FD systems without the proposed ASE model are introduced as a baseline to compare it with the FD system using the ASE model. The detection performance of the FD systems using k -NN and SVM models with different sampling rates in the SisFall and FallAllID datasets are shown in Fig. 2 and Fig. 3, where “kNN_ordinal” is the typical FD system using k -NN model without the proposed ASE model, and “kNN_enhanced” is the k -NN-based FD system with the enhanced accelerometer signal. The “SVM_ordinal” and “SVM_enhanced” have similar definitions. Generally, applying the ASE model to FD systems improve the system performance in most sampling rates and evaluation metrics, especially accuracy and sensitivity. Moreover, the proposed ASE model has more positive effects when the sampling rate is lower. Particularly, the FD systems using SVM and ASE models outperform systems with other models at most sampling rates. The results show that the SVM-based FD systems with ASE models at the lowest sampling rate achieved 97.34% ACC in SisFall and 90.52% ACC in FallAllID, while that without ASE models only achieved 95.92% ACC in SisFall and 87.47% ACC in FallAllID.

The best detection results of the FD systems with and without ASE are listed in TABLE V and TABLE VI, respectively. As evident from the two tables, the best detection performance is slightly improved using the proposed ASE model, especially for SVM models. The best accuracy of the FD systems using the ASE model achieved 99.41% for SisFall and 95.6% for

TABLE VI

THE BEST PERFORMANCE USING TYPICAL WEARABLE FD SYSTEMS WITH AND WITHOUT THE ASE MODEL IN FALLALLID DATASET (%).

	kNN	original kNN	enhanced SVM	original SVM	enhanced
Accuracy	94.11	93.97	94.58	95.60	
Sensitivity	87.00	90.31	88.89	90.31	
Specificity	96.96	95.54	96.96	97.72	
Precision	92.00	89.02	92.12	94.09	

FallAllID.

The detailed detection performance at the lowest sampling rate in SisFall (1.56 Hz) and FallAllID (1.86 Hz) datasets for each fall and ADL type are presented in Fig. 4, Fig. 5, and Fig. 6. For the SisFall dataset, most types improved, especially F05, “Fall forward while jogging, caused by a trip”, A06 “Walking upstairs and downstairs quickly”, and A13 “Sitting a moment, lying quickly, waiting a moment, and sitting again”. However, the ASE model has negative effects when the FD systems tackle A03 “Jogging slowly”. There are more than 10 types of falls and ADL showing at least 10% improvement in the FallAllID dataset, but the FD systems dramatically worsened its detection performance for three types, F27, F28, and A25.

V. DISCUSSION

The results reveal that the accuracy of the typical FD systems without the proposed ASE model decreases significantly when the sampling rate is less than 6.25 Hz in SisFall and 14.88 Hz in FallAllID. These results are similar to those of previous studies [19, 20]. This reduction in accuracy is owed to the loss of important information and critical movement patterns in LR signals. As shown in Fig. 7 and Fig. 8, the accelerometer signal degrades significantly when the sampling rate decreases from the initial sampling rate (Raw-200 Hz) to an extremely low sampling rate (Downsampled-1.56 Hz). Moreover, it leads to several technical challenges for FD systems such as misalignment, mismatch of the effective features, and degradation effects.

To deal with these challenges, an ASE model is proposed to reconstruct the accelerometer signal from LR to HR. As presented in Fig. 7, several important movement features of the fall signal (Enhanced-1.56 Hz) are reconstructed using the proposed ASE model such as impact, free-fall, and vibration. The reconstructed signal can help FD systems accurately align the impact point of the fall signal and tackle the mismatch problems of the effective features. Fig. 8 demonstrates that the enhanced ADL patterns are more similar to a fall than an ADL signal. However, the enhanced signal still enables the FD system to achieve better detection performance. Moreover, the proposed ASE model has positive effects on HR-FD systems, as shown in TABLE V and TABLE VI. It filters the noise (e.g., muscle vibration) and keep the motion patterns, which improves the ability of the FD system to classify falls and ADL.

As shown in Figs. 4, 5, and 6, the results show that the FD systems using the proposed ASE model show significant improvement in several types of falls and ADL, such as “sitting on a chair”. However, the FD system with the ASE model is still weak in “lying on the bed” and “lateral fall while lying”.

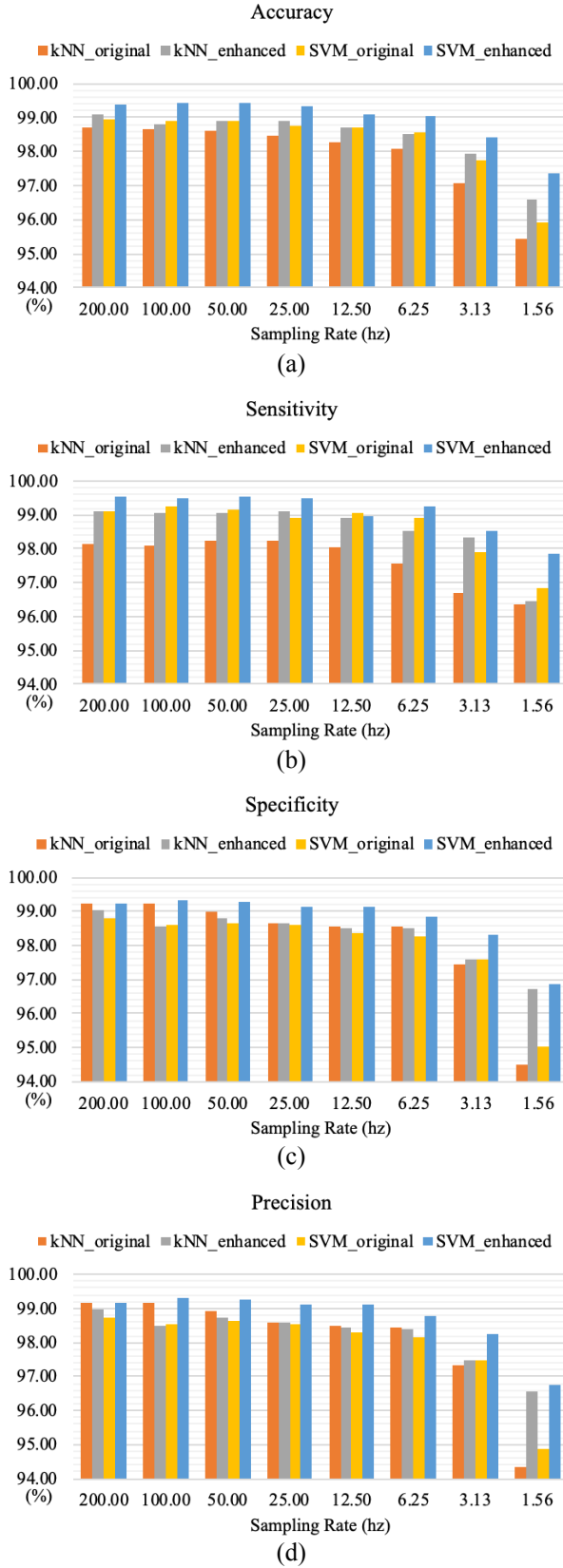


Fig. 2 (a) ACC, (b) SEN, (c) SPE, and (d) PRE of sampling rates vs typical wearable FD systems with ASE and without ASE in SisFall dataset.

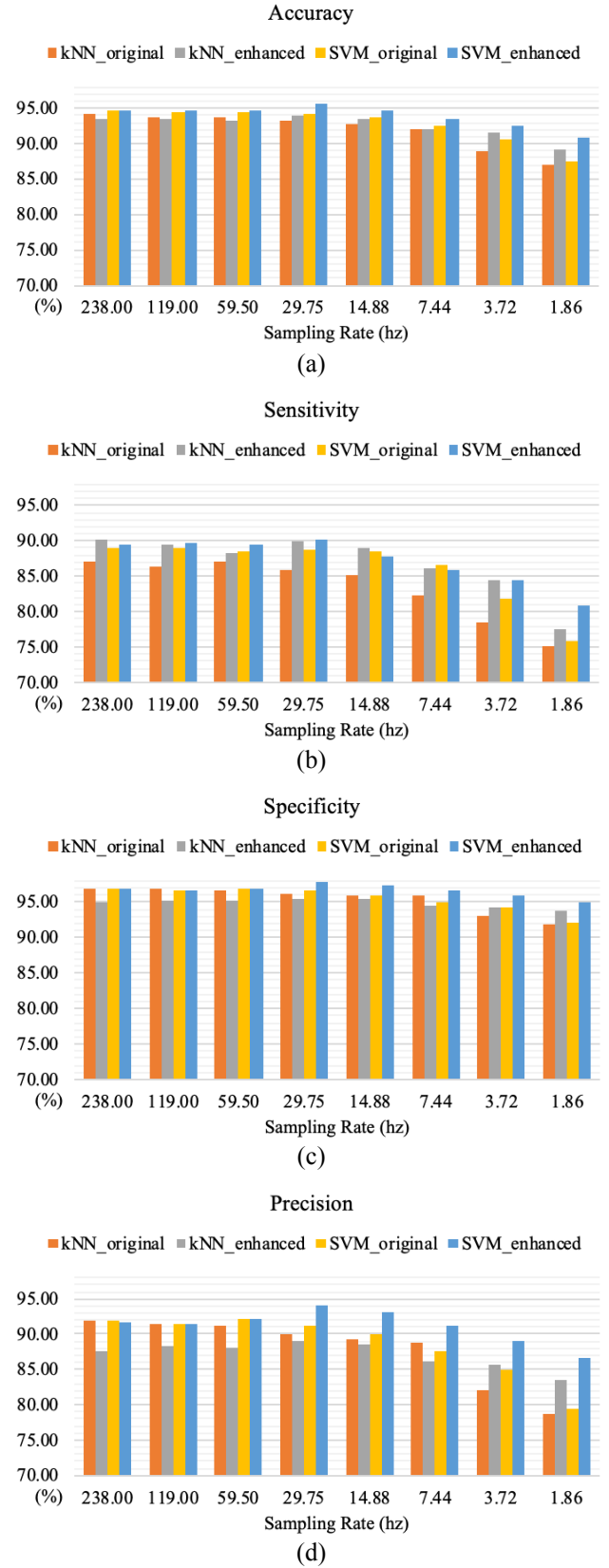


Fig. 3 (a) ACC, (b) SEN, (c) SPE, and (d) PRE of sampling rates vs typical wearable FD systems with ASE and without ASE in FallAIID dataset.

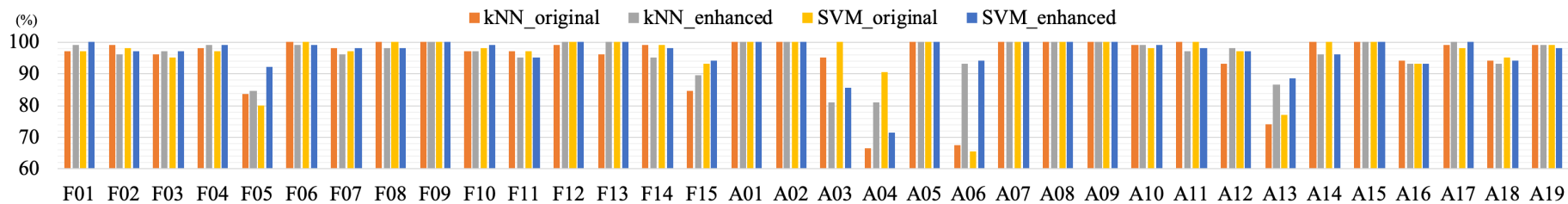


Fig. 4 The detection sensitivity and precision of SisFall dataset for each fall and ADL type at the sampling rate of 1.56 Hz.

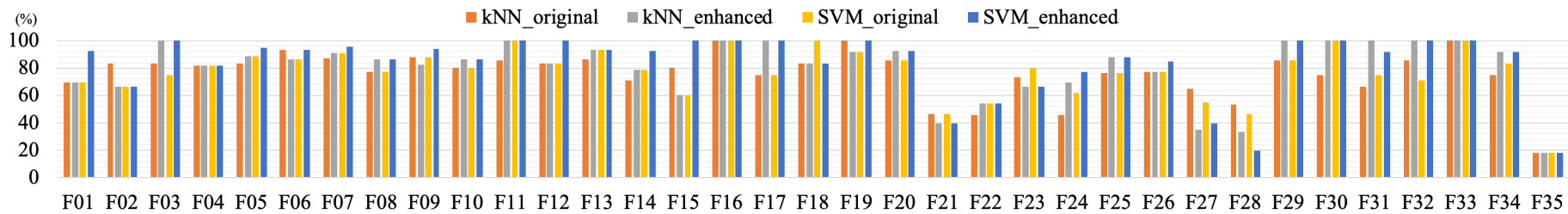


Fig. 5 The detection sensitivity of FallAIID dataset for each fall type at the sampling rate of 1.86 Hz.

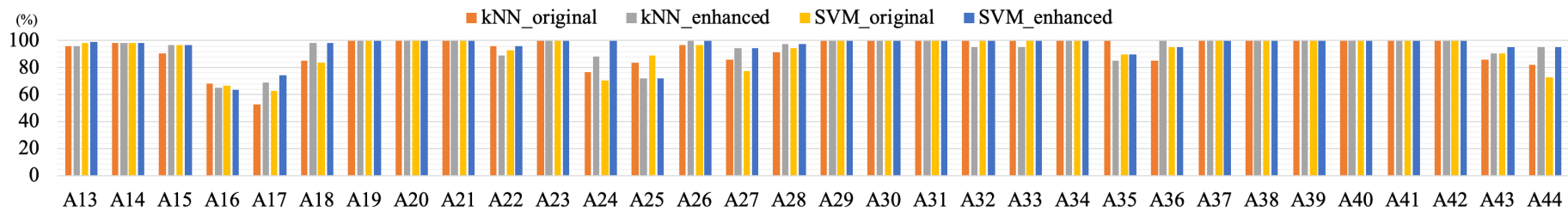


Fig. 6 The detection precision of FallAIID dataset for each ADL type at the sampling rate of 1.86 Hz.

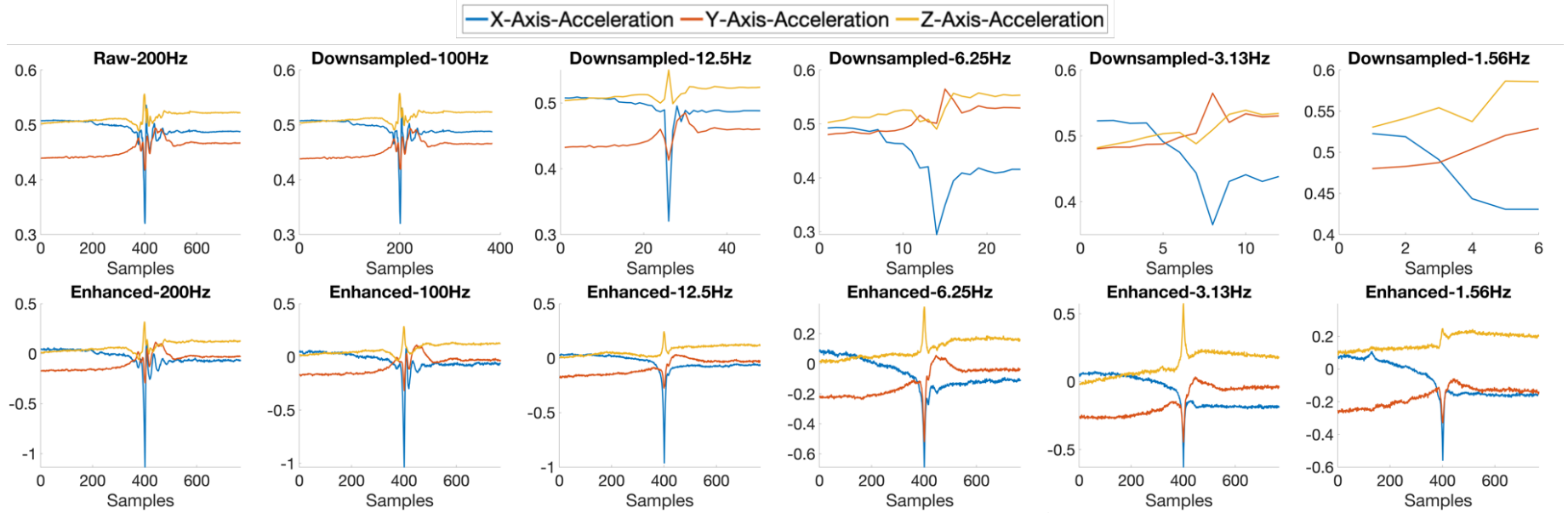


Fig. 7 An example signal of the ASE model on F14 "Fall backward while sitting, caused by fainting or falling asleep" in SisFall dataset. The 1st row shows the raw accelerometer signal and the LR signal with different downsampled sizes. The 2nd row shows the reconstructed signal using the proposed ASE model.

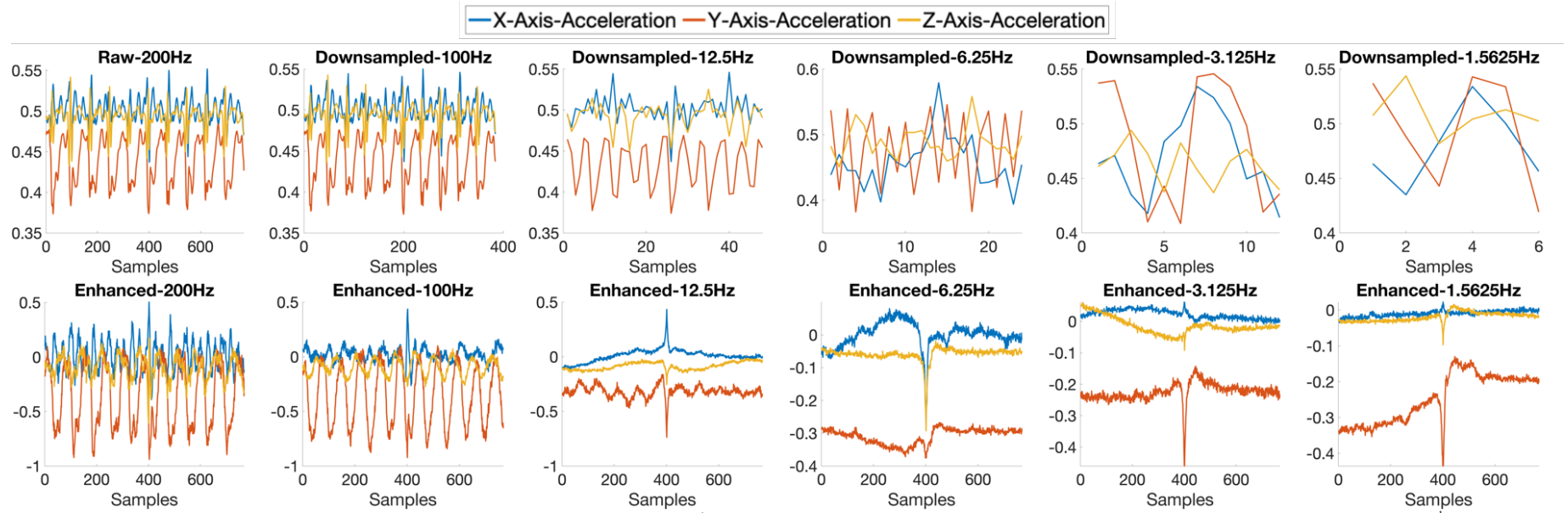


Fig. 8 An example signal of the ASE model on A03 "Jogging slowly" in SisFall dataset. The 1st row shows the raw accelerometer signal and the LR signal with different downsampled sizes. The 2nd row shows the reconstructed signal using the proposed ASE model.

This is owing to the fact that the important movement is still missing in the reconstructed signal. Moreover, it may worsen the detectability of the FD system, such as “jogging slowly” in SisFall, and “jogging quickly” in FallAIIID. To enhance the reconstruction capability, a more powerful neural network model will be implemented in future studies such as generative adversarial network (GAN) [34].

To the best of our knowledge, this is the first study focused on improving the performance of LR-FD systems using the DL-based ASE model. A similar signal enhancement approach has been successfully implemented in other fields such as face recognition [35] and speech recognition [36]. For a typical FD system, the proposed ASE model could be a front-end processor to enhance the LR signal before further processing. The results demonstrate that the ASE model enables LR-FD systems to achieve better detection accuracy. Additionally, the extra computational cost of the ASE model is acceptable and valuable for FD systems as the power consumption of the data sampling is much greater than any other processes, even using machine learning or deep learning models [23, 24].

Previous studies have applied other power-saving techniques to FD systems that achieved over 90% detection performance [17, 18, 37]. However, it is difficult to directly compare this study as a design principle as the target of this study is different from those studies. They employed adaptive sampling rates to avoid the negative effects of the LR signal on FD systems, while we aim to directly enhance the LR-FD system using the DL-based ASE model. In fact, the proposed ASE model can be incorporated into their studies to potentially achieve better system performance. Furthermore, their energy-efficient mechanisms are validated on private datasets. Therefore, we use two public datasets, SisFall and FallAIIID, to explore the effectiveness of the proposed ASE model on FD systems instead of using a nonpublic dataset. The detection performance of the FD system without the ASE model was the reference.

The main limitation of this study is that the applied open datasets involve emulated fall events and ADL performed by healthy young subjects rather than real-world data from elder people. Their movement characteristics and features are significantly different from those of the emulated experiments [38]. This may lead to the model, trained with the emulated data, to perform worse on real-world data [39]. Therefore, a real-world dataset (e.g., FARSEEING [40]) will be included to validate the effectiveness of the proposed ASE model on FD systems.

VI. CONCLUSION

A practical power-saving approach to develop energy-efficient FD systems in a real-world environment is to decrease the sampling rate. However, low sampling rate leads to LR accelerometer signals for FD systems. The detection accuracy significantly decreases when the sampling frequency is less than 10 Hz. To enhance the performance of LR-FD systems, technical challenges such as misalignment, mismatch of effective features, and degradation effect, require further

investigation. In this study, we propose a DL-based ASE model that reconstructs the HR signal from the LR signal by learning the relationship and correlation between the LR and HR signals. The predicted fine-grained movement information from the enhanced accelerometer signal enables LR-FD systems to tackle technical challenges and achieve better performance. The results show that the SVM-based FD systems using the DL-based ASE model at an extremely low sampling rate (SisFall: 1.56 Hz and FallAIIID: 1.86 Hz) achieved 97.34% and 90.52% ACC in SisFall and FallAIIID, respectively, whereas that without ASE models only achieved 95.92% and 87.47% ACC in SisFall and FallAIIID, respectively. This study demonstrates the effectiveness of the ASE model on LR-FD systems.

REFERENCE

- [1] S. Yoshida, "A global report on falls prevention epidemiology of falls," 2007.
- [2] M. E. Tinetti, W. L. Liu, and E. B. Claus, "Predictors and prognosis of inability to get up after falls among elderly persons," (in eng), *Jama*, vol. 269, no. 1, pp. 65-70, Jan 6 1993.
- [3] D. Wild, U. S. Nayak, and B. Isaacs, "How dangerous are falls in old people at home?," (in eng), *Br Med J (Clin Res Ed)*, vol. 282, no. 6260, pp. 266-8, Jan 24 1981, doi: 10.1136/bmj.282.6260.266.
- [4] P. Vallabh and R. Malekian, "Fall detection monitoring systems: a comprehensive review," *Journal of Ambient Intelligence and Humanized Computing*, vol. 9, no. 6, pp. 1809-1833, 2018/11/01 2018, doi: 10.1007/s12652-017-0592-3.
- [5] D. Yacchirema, J. S. de Puga, C. Palau, and M. Esteve, "Fall detection system for elderly people using IoT and ensemble machine learning algorithm," *Personal and Ubiquitous Computing*, vol. 23, no. 5, pp. 801-817, 2019/11/01 2019, doi: 10.1007/s00779-018-01196-8.
- [6] C. Y. Hsieh, K. C. Liu, C. N. Huang, W. C. Chu, and C. T. Chan, "Novel Hierarchical Fall Detection Algorithm Using a Multiphase Fall Model," (in eng), *Sensors (Basel)*, vol. 17, no. 2, Feb 8 2017, doi: 10.3390/s17020307.
- [7] L. Yang, Y. Ren, and W. Zhang, "3D depth image analysis for indoor fall detection of elderly people," *Digital Communications and Networks*, vol. 2, no. 1, pp. 24-34, 2016/02/01/ 2016, doi: <https://doi.org/10.1016/j.dcan.2015.12.001>.
- [8] F. Harrou, N. Zerrouki, Y. Sun, and A. Houacine, "An Integrated Vision-Based Approach for Efficient Human Fall Detection in a Home Environment," *IEEE Access*, vol. 7, pp. 114966-114974, 2019, doi: 10.1109/ACCESS.2019.2936320.
- [9] Y. Zigel, D. Litvak, and I. Gannot*, "A Method for Automatic Fall Detection of Elderly People Using Floor Vibrations and Sound—Proof of Concept on Human Mimicking Doll Falls," *IEEE Transactions on Biomedical Engineering*, vol. 56, no. 12, pp. 2858-2867, 2009, doi: 10.1109/TBME.2009.2030171.
- [10] G. Feng, J. Mai, Z. Ban, X. Guo, and G. Wang, "Floor Pressure Imaging for Fall Detection with Fiber-Optic Sensors," *IEEE Pervasive Computing*, vol. 15, no. 2, pp. 40-47, 2016, doi: 10.1109/MPRV.2016.27.
- [11] F. Riquelme, C. Espinoza, T. Rodenas, J. G. Minonzio, and C. Taramasco, "eHomeSeniors Dataset: An Infrared Thermal Sensor Dataset for Automatic Fall Detection Research," (in eng), *Sensors (Basel)*, vol. 19, no. 20, Oct 21 2019, doi: 10.3390/s19204565.
- [12] N. Pannurat, S. Thiemjarus, and E. Nantajeewarawat, "Automatic fall monitoring: a review," (in eng), *Sensors (Basel)*, vol. 14, no. 7, pp. 12900-36, Jul 18 2014, doi: 10.3390/s140712900.
- [13] M. Chan, D. Estève, J. Y. Fourniols, C. Escriba, and E. Campo, "Smart wearable systems: current status and future challenges," (in eng), *Artif Intell Med*, vol. 56, no. 3, pp. 137-56, Nov 2012, doi: 10.1016/j.artmed.2012.09.003.
- [14] K. Bodine and F. Gemperle, "Effects of functionality on perceived comfort of wearables," in *Seventh IEEE International Symposium on Wearable Computers, 2003. Proceedings.*, 21-23 Oct. 2003 2003, pp. 57-60, doi: 10.1109/ISWC.2003.1241394.

- [15] L. Bloom, R. Eardley, E. Geelhoed, M. Manahan, and P. Ranganathan, "Investigating the Relationship Between Battery Life and User Acceptance of Dynamic, Energy-Aware Interfaces on Handhelds," Berlin, Heidelberg, 2004: Springer Berlin Heidelberg, in Mobile Human-Computer Interaction - MobileHCI 2004, pp. 13-24.
- [16] J. H. M. Bergmann and A. H. McGregor, "Body-Worn Sensor Design: What Do Patients and Clinicians Want?," *Annals of Biomedical Engineering*, vol. 39, no. 9, pp. 2299-2312, 2011/09/01 2011, doi: 10.1007/s10439-011-0339-9.
- [17] C. Wang *et al.*, "Low-Power Fall Detector Using Triaxial Accelerometry and Barometric Pressure Sensing," *IEEE Transactions on Industrial Informatics*, vol. 12, no. 6, pp. 2302-2311, 2016, doi: 10.1109/TII.2016.2587761.
- [18] C. Wang, W. Lu, S. J. Redmond, M. C. Stevens, S. R. Lord, and N. H. Lovell, "A Low-Power Fall Detector Balancing Sensitivity and False Alarm Rate," (in eng), *IEEE J Biomed Health Inform*, vol. 22, no. 6, pp. 1929-1937, Nov 2018, doi: 10.1109/jbhi.2017.2778271.
- [19] K. Liu, C. Hsieh, S. J. Hsu, and C. Chan, "Impact of Sampling Rate on Wearable-Based Fall Detection Systems Based on Machine Learning Models," *IEEE Sensors Journal*, vol. 18, no. 23, pp. 9882-9890, 2018, doi: 10.1109/JSEN.2018.2872835.
- [20] J. Silva, D. Gomes, I. Sousa, and J. S. Cardoso, "Automated Development of Custom Fall Detectors: Position, Model and Rate Impact in Performance," *IEEE Sensors Journal*, vol. 20, no. 10, pp. 5465-5472, 2020, doi: 10.1109/JSEN.2020.2970994.
- [21] C. Wang, S. J. Redmond, W. Lu, M. C. Stevens, S. R. Lord, and N. H. Lovell, "Selecting Power-Efficient Signal Features for a Low-Power Fall Detector," *IEEE Transactions on Biomedical Engineering*, vol. 64, no. 11, pp. 2729-2736, 2017, doi: 10.1109/TBME.2017.2669338.
- [22] J. He, Z. Zhang, X. Wang, and S. Yang, "A Low Power Fall Sensing Technology Based on FD-CNN," *IEEE Sensors Journal*, vol. 19, no. 13, pp. 5110-5118, 2019, doi: 10.1109/JSEN.2019.2903482.
- [23] X. Fafoutis, L. Marchegiani, A. Elsts, J. Pope, R. Piechocki, and I. Craddock, "Extending the battery lifetime of wearable sensors with embedded machine learning," in *2018 IEEE 4th World Forum on Internet of Things (WF-IoT)*, 5-8 Feb. 2018 2018, pp. 269-274, doi: 10.1109/WF-IoT.2018.8355116.
- [24] J. Kim and C. Chu, "Analysis of energy consumption for wearable ECG devices," in *SENSORS, 2014 IEEE*, 2-5 Nov. 2014 2014, pp. 962-965.
- [25] K. Liu, C. Hsieh, H. Huang, S. J. Hsu, and C. Chan, "An Analysis of Segmentation Approaches and Window Sizes in Wearable-Based Critical Fall Detection Systems With Machine Learning Models," *IEEE Sensors Journal*, vol. 20, no. 6, pp. 3303-3313, 2020, doi: 10.1109/JSEN.2019.2955141.
- [26] A. T. Özdemir, "An Analysis on Sensor Locations of the Human Body for Wearable Fall Detection Devices: Principles and Practice," (in eng), *Sensors (Basel)*, vol. 16, no. 8, Jul 25 2016, doi: 10.3390/s16081161.
- [27] A. Sucerquia, J. D. López, and J. F. Vargas-Bonilla, "SisFall: A Fall and Movement Dataset," (in eng), *Sensors (Basel)*, vol. 17, no. 1, Jan 20 2017, doi: 10.3390/s17010198.
- [28] R. L. B. J. Majd SALEH, FallAllID: A Comprehensive Dataset of Human Falls and Activities of Daily Living [Online] Available: <http://dx.doi.org/10.21227/bnya-mn34>
- [29] E. Casilari, J. A. Santoyo-Ramón, and J. M. Cano-García, "UMAFall: A Multisensor Dataset for the Research on Automatic Fall Detection," *Procedia Computer Science*, vol. 110, pp. 32-39, 2017/01/01/ 2017, doi: <https://doi.org/10.1016/j.procs.2017.06.110>.
- [30] L. Martínez-Villaseñor, H. Ponce, J. Brieva, E. Moya-Albor, J. Núñez-Martínez, and C. Peñafort-Asturiano, "UP-Fall Detection Dataset: A Multimodal Approach," *Sensors*, vol. 19, no. 9, p. 1988, 2019. [Online]. Available: <https://www.mdpi.com/1424-8220/19/9/1988>.
- [31] K. Liu, C. Hsieh, H. Huang, L. Chiu, S. J. Hsu, and C. Chan, "Drinking Event Detection and Episode Identification Using 3D-Printed Smart Cup," *IEEE Sensors Journal*, pp. 1-1, 2020, doi: 10.1109/JSEN.2020.3004051.
- [32] K. Liu, C. Hsieh, and C. Chan, "Transition-Aware Housekeeping Task Monitoring Using Single Wrist-Worn Sensor," *IEEE Sensors Journal*, vol. 18, no. 21, pp. 8950-8962, 2018, doi: 10.1109/JSEN.2018.2868278.
- [33] A. T. Özdemir and B. Barshan, "Detecting Falls with Wearable Sensors Using Machine Learning Techniques," *Sensors*, vol. 14, no. 6, pp. 10691-10708, 2014. [Online]. Available: <https://www.mdpi.com/1424-8220/14/6/10691>.
- [34] I. Goodfellow *et al.*, "Generative adversarial nets," in *Advances in neural information processing systems*, 2014, pp. 2672-2680.
- [35] Z. Wang, Z. Miao, Q. M. Jonathan Wu, Y. Wan, and Z. Tang, "Low-resolution face recognition: a review," *The Visual Computer*, vol. 30, no. 4, pp. 359-386, 2014/04/01 2014, doi: 10.1007/s00371-013-0861-x.
- [36] X. Li, V. Chebiyyam, and K. Kirchhoff, *Speech Audio Super-Resolution For Speech Recognition* (Proc. Interspeech 2019). 2019.
- [37] L. Zheng *et al.*, "A Novel Energy-Efficient Approach for Human Activity Recognition," (in eng), *Sensors (Basel)*, vol. 17, no. 9, Sep 8 2017, doi: 10.3390/s17092064.
- [38] F. Bagalà *et al.*, "Evaluation of accelerometer-based fall detection algorithms on real-world falls," (in eng), *PLoS One*, vol. 7, no. 5, p. e37062, 2012, doi: 10.1371/journal.pone.0037062.
- [39] J. Sims, K. Hill, S. Davidson, J. Gunn, and N. Huang, "A snapshot of the prevalence of physical activity amongst older, community dwelling people in Victoria, Australia: patterns across the 'young-old' and 'old-old'," (in eng), *BMC Geriatr*, vol. 7, p. 4, Feb 23 2007, doi: 10.1186/1471-2318-7-4.
- [40] J. Klenk *et al.*, "The FARSEEING real-world fall repository: a large-scale collaborative database to collect and share sensor signals from real-world falls," (in eng), *Eur Rev Aging Phys Act*, vol. 13, p. 8, 2016, doi: 10.1186/s11556-016-0168-9.